Radiative rate modification in CdSe quantum dot-coated microcavity

Aneesh V. Veluthandath and Prem B. Bisht

Citation: Journal of Applied Physics **118**, 233102 (2015); doi: 10.1063/1.4937577
View online: http://dx.doi.org/10.1063/1.4937577
View Table of Contents: http://aip.scitation.org/toc/jap/118/23
Published by the American Institute of Physics

Radiative rate modification in CdSe quantum dot-coated microcavity

Aneesh V. Veluthandath and Prem B. Bisht[a)]
Department of Physics, Indian Institute of Technology Madras, Chennai 600036, India

(Received 28 August 2015; accepted 29 November 2015; published online 15 December 2015)

Whispering gallery modes (WGMs) of the microparticles with spherical or cylindrical symmetry have exceptionally high quality factors and small mode volume. Quantum dots (QDs) are zero dimensional systems with variable band gap as well as luminescent properties with applications in photonics. In this paper, the WGMs have been observed in the luminescence spectra of CdSe QD-coated single silica microspheres. Theoretical estimations of variation of resonance frequency, electric field, and Q-values have been done for a multilayer coating of QDs on silica microspheres. Observed WGMs have been identified for their mode number and polarization using Mie theory. Broadening of modes due to material absorption has been observed. Splitting of WGMs has also been observed due to coherent coupling of counter propagating waves in the microcavity due to the presence of QDs. At room temperature, the time-resolved study indicates the modification of the radiative rate due to coupling of WGMs of the microcavity-QD hybrid system. © *2015 AIP Publishing LLC*. [http://dx.doi.org/10.1063/1.4937577]

I. INTRODUCTION

Light trapped in a dielectric microsphere can result in the observation of sharp resonances called whispering gallery modes (WGMs) or morphology dependent resonance.[1] These microcavity resonances exhibit quality factors of the order of 10^4–10^9 and have a low mode volume.[2] The resonance frequencies and Q values of the WGMs depend on the size of the microcavity as well as on the refractive index contrast between the microresonator and the surrounding medium. WGMs have found applications in low threshold microlasers,[3] add-drop filters,[4] and refractive index sensors.[5] Fluorescence based WGM refractive index sensors gained attention due to their simplicity and robustness.[6] The high refractive index fluorescent layer used on sensors is known to increase the sensitivity.[7]

Quantum dots (QDs) are semiconductor nanocrystals of high refractive index with sizes less than 10 nm.[8] Energy levels of QDs are quantized, and hence sometime these are referred as artificial atoms. As the motion of the electrons is confined in 3D, the QDs exhibits properties intermediate to the bulk material and that of the single molecule.[9] Optical and electronic properties of QDs can be tuned by controlling their size[10,11] for novel optoelectronic and electric devices.[12,13] QD based devices such as flash memories,[14] photodetectors,[15] light emitting diodes,[16] and microlasers[17,18] have been demonstrated. QDs are also finding applications in solar energy harvesting.[19]

WGMs have been observed in dye embedded microspheres.[20–23] However, organic dyes are susceptible to photobleaching. QDs are proposed as an attractive alternative to organic dyes due to their higher photostability.[24] In recent years, WGMs have been observed in photoluminescence (PL) and Raman spectra of QD-coated microspheres.[25,26] QD coupled WGM based refractive index sensors were demonstrated by measuring the WGM shift.[5,27] QD coupled WGM lasers have also been demonstrated.[28–30]

If an emitter is kept in the vicinity of a dielectric microcavity, its transition moment can be modified following the Fermi's golden rule.[9] The radiative rate can either be enhanced[9,31–33] or inhibited[34,35] depending on the fact whether the emission spectrally coincides with the resonance peak or the valley of WGM resonances. Lin *et al.*[36] measured the radiative rate enhancement and inhibition of chelated europium ions in falling droplets of dimethylformamide. There is a significant amount of literature on WGM modified radiative rate and energy transfer of organic dyes.[22,37–41] Purcell regime of QDs coupled WGMs can be exploited for various applications such as single photon source and amplified spontaneous emission. To observe the Purcell enhancement, the natural line width of the QDs should be less than the free spectral range (FSR) of the microcavity.[42] The WGMs in QD-microsphere systems have been studied by Gaponik *et al.*[25] The CdSe QDs have a line width of a few cm^{-1} at low temperatures.[43] Due to phonon interactions, the natural line width of QDs increases with temperature.[44] A few studies on Purcell enhancement of CdSe QD coupled-WGM resonators have been done at cryogenic temperatures.[43,45] However, studies on the rate modification at higher temperature do not exist in the literature. From the point of view of technological relevance, such studies may help fabricate cavity-QED based devices and hybrid sensors.[46] In view of the above, we report here the spontaneous emission rate enhancement of CdSe QDs coupled WGMs of single microcavity at room temperature.

II. EXPERIMENTAL

Commercially available sample of colloidal quantum dots (MKN-CdSe-T500) dispersed in toluene was used as-received. The characterization of QDs in solution by steady state spectra was done by using a dual beam UV-Visible spectrometer (JASCO, V-570) and a spectrofluorometer

a)E-mail: bisht@iitm.ac.in

(JASCO, FP-6600). The preparation of CdSe QDs coated microspheres was done in a manner suggested by Finlayson *et al.*[47] In brief, the silica microspheres were treated with 10% hexamethyldisilazane (HMDS) in methanol for half an hour. The toluene solution of CdSe QDs was added to the treated microspheres dispersed in 2-propanol. The mixture was sonicated for 5 min and was kept in ambient conditions for the next 24 h to let the QDs precipitate on the microspheres. The microspheres were centrifuged and washed with 2-propanol and toluene, respectively, to remove the excess QDs. The QDs coated microspheres were kept on a clean glass plate for measurements. PL from the single microsphere was measured using a micro-Raman spectrometer (HR800UV, Horiba Jobin Yvon) with the excitation wavelength of argon ion laser (488 nm).

The luminescence lifetimes were measured with the time-correlated single photon counting (TCSPC) technique under a fluorescence microscope (Nikon 80i). A 40 ps diode laser with a center wavelength of 470 nm (Pil047, Advance Photon system) was used for excitation. Emitted light was detected using a photomultiplier tube (Hamamatsu, R298). The system was calibrated by measuring the fluorescence decay of rhodamine 6G in methanol as a standard. Commercially available software TC900 and FAST (Edinburgh Instruments) were used in data collection and analysis, respectively. The goodness of the fit was judged by using the residuals and the χ^2 value. For a good fit, the χ^2 was around one, and residuals were distributed evenly about the zero line. Axisym method[48] implemented in Comsol multiphysics (4.3b) was used to simulate layered microspheres. The scattering efficiency for a microcavity was obtained by using the programs of Bohran and Huffman.[49,50]

III. THEORETICAL ASPECTS

A. Scattering efficiency of a microcavity

The resonance frequency and the Q-values of WGMs in a layered microsphere can be calculated using the Aden-Kerker theory.[22,51,52] Refractive indices of the microsphere (of radius r) and coating layer (of thickness t) are denoted as m_1 and m_2, respectively. The scattering efficiency of the layered microsphere is given as

$$Q_{sca} = \frac{2\pi}{|k|^2}\sum_{n=1}^{\infty}(2n+1)\left(|a_n^s|^2 + |b_n^s|^2\right), \tag{1}$$

where k is complex propagation constant and n is called the mode number. The a_n^s and b_n^s are given as[51,52]

$$a_n^s = \frac{\psi_n(x_2)\left[\psi_n'(m_2x_2) - A_n\chi_n'(m_2x_2)\right] - m_2\psi_n'(x_2)\left[\psi_n(m_2x_2) - A_n\chi_n(m_2x_2)\right]}{\xi_n(x_2)\left[\psi_n'(m_2x_2) - A_n\chi_n'(m_2x_2)\right] - m_2\xi_n'(x_2)\left[\psi_n(m_2x_2) - A_n\chi_n(m_2x_2)\right]}, \tag{2a}$$

$$b_n^s = \frac{m_2\psi_n(x_2)\left[\psi_n'(m_2x_2) - B_n\chi_n'(m_2x_2)\right] - \psi_n'(x_2)\left[\psi_n(m_2x_2) - B_n\chi_n(m_2x_2)\right]}{m_2\xi_n(x_2)\left[\psi_n'(m_2x_2) - B_n\chi_n'(m_2x_2)\right] - \xi_n'(x_2)\left[\psi_n(m_2x_2) - B_n\chi_n(m_2x_2)\right]}, \tag{2b}$$

where $x_2 = k(r+t)$ and ψ_n, χ_n, and ξ_n are Riccati-Bessel functions related to their spherical counter parts through the relations

$$\psi_n(z) = xj_n(z),\ \chi_n(z) = -xn_n(z), \quad \text{and} \quad \xi_n(z) = xh_n^{(1)}(z).$$

The A_n and B_n are evaluated at the interface between the microsphere and the coating layer and are given as

$$A_n = \frac{m_2\psi_n(m_2x)\psi_n'(m_1x) - m_1\psi_n'(m_2x)\psi_n(m_1x_1)}{m_2\chi_n(m_2x)\psi_n'(m_1x) - m_1\chi_n'(m_2x)\psi_n(m_1x)}, \tag{3a}$$

$$B_n = \frac{m_2\psi_n(m_1x)\psi_n'(m_2x) - m_1\psi_n'(m_1x)\psi_n(m_2x)}{m_2\chi_n'(m_2x)\psi_n(m_1x) - m_1\psi_n'(m_1x)\chi_n(m_2x)}, \tag{3b}$$

where $x = kr$ is known as the x-parameter. In case of a homogeneous sphere, the A_n and B_n coefficients vanish and the a_n^s and $b_n{}^s$ become corresponding Mie coefficients.[22]

WGMs are identified by the mode number (n) and mode order (m). While n is the number of wavelengths that fit into the circumference of the microsphere, m is the number of nodes along the radial direction. For a TM_{40} mode, simulated images of first and second order modes are given in Figure 1. As can be seen, there are 40 spots near the periphery of the microsphere, each corresponding to a half wavelength ($\lambda/2$). The FSR is defined as the frequency spacing between two successive modes of same polarization and mode order.

B. Purcell effect in a microcavity

According to Fermi's golden rule,[53] the radiative rate of a dipole can be different from its free space value. The new

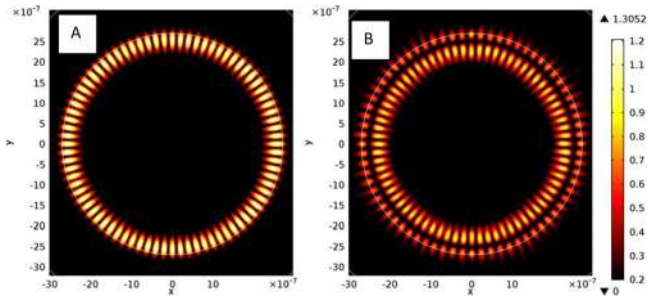

FIG. 1. Simulations of WGMs in equatorial plane of a microsphere with radius (r) = 2.7 μm and refractive index (m_1) = 1.48 for the TM mode with n = 40, and mode orders m = 1 (a) and m = 2 (b).

rate (Γ_{cav}) when the emitter is in resonance with cavity field is given as

$$\Gamma_{cav} = \frac{3}{4\pi^2}\left(\frac{Q}{V_{eff}}\right)\lambda_0^3\Gamma_0, \tag{4}$$

where Γ_0 is the free space value of the radiative rate, V_{eff} is the effective mode volume or the volume occupied by a particular resonator mode under consideration, and λ_0 is the free space wavelength of the mode. The radiative rate is enhanced by a factor known as Purcell factor (F_p)[54]

$$F_p = \frac{\Gamma_{cav}}{\Gamma_0} = \frac{3}{4\pi^2}\left(\frac{Q}{V_{eff}}\right)\lambda_0^3. \tag{5}$$

According to Yokoyama and Brorson,[42] the following three conditions are required to observe the modification of the radiative rate: (i) the Q-factor of the cavity should be sufficiently large, (ii) V_{eff} should be small, and (iii) the line width of the emitter preferably be small compared with the FSR of WGMs.

C. Effect of coating thickness of QDs on microcavity

The coating of QDs on a microsphere acts as a high refractive index layer that drags the electric field further towards the periphery.[55] A typical simulation of electric field variation is shown in Figure 2. By assuming a multilayer coating of QDs with average size as 2.2 nm, a silica microsphere with a diameter of 5.9 μm has been used for simulations for a first order TM_{44} mode.

The variation of the resonance frequency as a function of the coating layer is also shown in Fig. 2(B). It can be seen that the resonance frequency of the WGM decreases with the coating thickness and the shift is larger for the TE mode. The ratio of this frequency shift to the FSR is known as figure of merit of tunability.[56] Such coating dependent shifts in WGMs are useful in sensitive sensing applications.

The Q values of both TE and TM modes also increase on increasing the coating thickness[57] (Figure 3(A)). However, the Q values of the TE modes increase rapidly than those of the TM modes. The refractive index of a material is a complex quantity. It is represented as $\eta + i\kappa$, where η is the real part and κ is the imaginary component of the refractive index. κ is responsible for the material absorption. In the presence

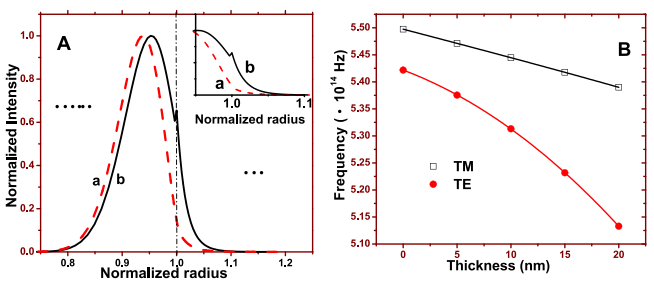

FIG. 2. (A) Effect of QD coating on silica microsphere of $r = 2.95\,\mu$m and $m_1 = 1.48$ for $t = 0$ (a) and $t = 10$ nm with $m_2 = 2.5$ (b). Electric field intensity along the radial direction is plotted for $TM_{44,1}$ mode. The inset shows the field near the surface of the sphere on expanded scale. (B) shows the effect of thickness on the peak frequency of the first order TE (●) and TM (□) modes.

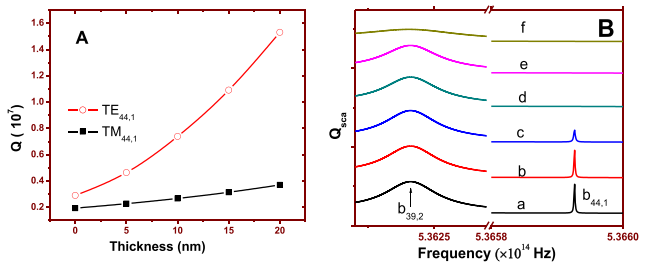

FIG. 3. Variation of Q factor of modes of the microsphere of r = 2.95 μm and $\eta = 1.48$ as a function of nanolayer thickness. The refractive index of the coating layer is 2.5 (A). (B) shows the scattering efficiency as a function of κ of the coating layer with a thickness of 5 nm. The κ values are (a) 0, (b) 5×10^{-7}.(c) 10^{-5}, (d) 5×10^{-4}, (e)10^{-3}, and (f) 10^{-2}. Scattering spectra have been offseted for brevity of presentation. The peak frequency of $b_{44,1}$ mode is 5.36593×10^{14} Hz.

of the material absorption, the total quality factor of the resonator (Q_{tot}) becomes

$$\frac{1}{Q_{tot}} = \frac{1}{Q_{rad}} + \frac{1}{Q_{mat}}, \tag{6}$$

where Q_{rad} is the radiation loss and Q_{mat} is due to material absorption and Rayleigh scattering.[58]

To further determine the effect of the absorption in the nanolayer, the scattering efficiency has been calculated as a function of κ (Fig. 3(B)). It is observed that the absorption leads to the reduction in scattering amplitude as well as the Q-value of the resonances. However, the effect of absorption is not so prominent on the higher order modes. The first order resonances disappear rapidly with subsequent reduction in their Q values for the κ value in the order of 10^{-3}, whereas the second order resonances survive even up to the κ value of 10^{-1}.

IV. RESULTS AND DISCUSSION

A. Steady state measurements and characterization of QDs

The absorption and PL spectra of colloidal solution of QD in toluene are given in Figure 4. The absorption peak is observed at 523.4 nm. The absorption spectrum has the full width at half maximum (fwhm) of 1666 cm^{-1}. The PL maximum occurs at 536 nm and has a fwhm of 1192 cm^{-1}. A Tauc plot has been used to estimate the energy band gap as follows. For a direct band gap semiconductor, $(\alpha h\nu)^{1/2}$ is plotted as a function of energy ($h\nu$). Here, α is the absorption

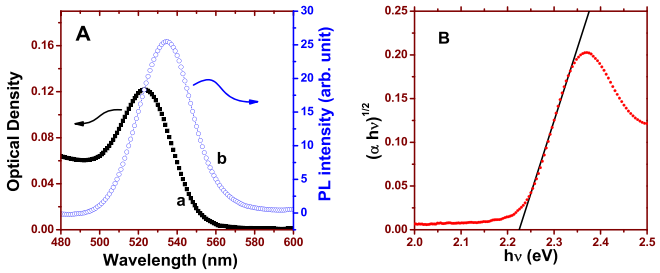

FIG. 4. Absorption (a) and PL spectrum (b) of CdSe QDs in toluene (A). Excitation wavelength is 470 nm. (B) shows the Tauc plot; here α is the absorption coefficient.

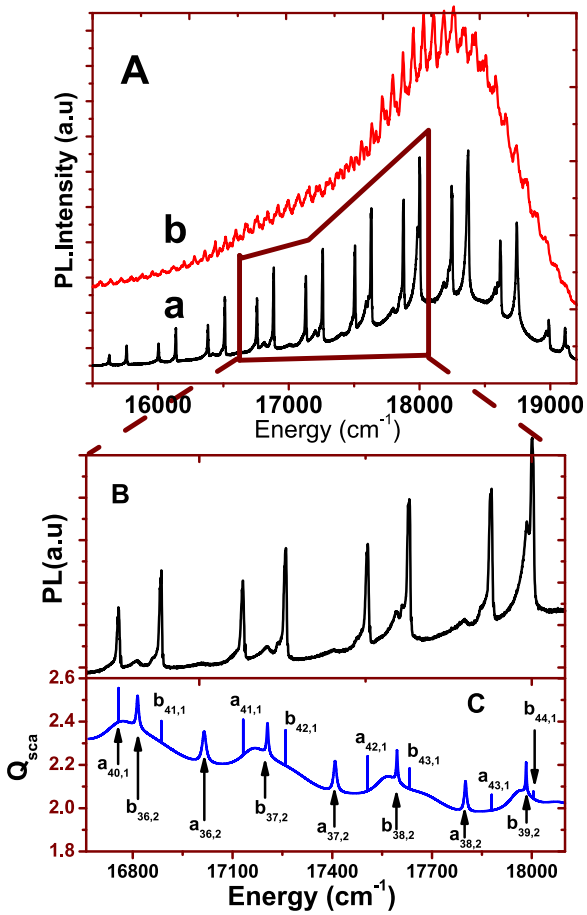

FIG. 5. Experimentally observed WGMs (A) in PL of CdSe coated microspheres with diameters of 6 μm (a) and 8 μm (b). (B) shows the expanded portion of curve (a) fitted with eq. 1 (C). The parameters of the fitting are $m_1 = 1.4891$, $r = 2.955$ μm, t = 2.2. nm with $m_2 = 2.2$ nm.

coefficient that can be estimated from the optical density (OD) using the relation $\alpha = 2.303 \times OD/d$, where d is the thickness of sample.[59] A straight line is fitted on the plotted curve. The x-intercept of the fitted straight line gives the band gap energy of 2.2 eV. This value falls within the literature values reported for CdSe quantum dots.[60,61]

B. Cavity effects

1. Observation of WGMs in luminescence spectrum

Figure 5 shows the PL spectra for QD-coated single microspheres. The spectra exhibit peaks built upon the PL of CdSe QDs. The number of peaks in the spectrum of 8 μm diameter microsphere is higher compared with that of 6 μm. This is because the FSR decreases with the increase in the size. A portion of the 6 μm diameter microsphere spectrum has been fitted with Aden-Kerker theory and is shown in the bottom panel. A single layer of QDs is assumed in the present case. It can be seen that the WGMs with first order are sharp, while broader peaks are observed for the second order WGMs. The spectra consist of both the TE and the TM modes. The intensity of the TE modes is higher than that of the TM modes. In this way, the structured PL spectra of QDs are characteristic by their coupling with the WGMs of the microcavity.

2. Effect of absorption and splitting of modes

The effect of material absorption can be seen in the frequency range of 18 500 cm^{-1} to 19 000 cm^{-1}. The fwhm of the WGMs are higher in this range as compared with longer wavelength region due to self-absorption by the QDs. While the theoretically simulated Q values are of the order of 10^6, a reduction in the Q-values is observed by a factor of 10^3. This reduction in Q value can be attributed to the absorption quality factor (Q_{mat}) as discussed above (vide supra, Figure 3(B)). The absorption also reduces the amplitude of the WGMs.

A Rayleigh scatterer on the microsphere can coherently couple the two counter propagating waves in the WGMs.[62] A scatterer lifts the degeneracy of these modes. This leads to the splitting of first order modes[62] present in the periphery (Fig. 1(a)). In the present case, QD itself acts as the scatterer that couples the two degenerate counter propagating waves. A further expanded portion of a typical mode ($TM_{43,1}$) is shown in Figure 6. Two peaks can be seen in the experimental spectra in contrast to the single peak predicted by the scattering theory. The mode can be fitted with a composite line of two Gaussian functions. It can be seen that the combined broad peak ($Q = 1.81 \times 10^3$) can be expressed as a sum of two lines with higher Q values. Similar splitting has been reported by Gaponik *et al.*[25] The weak side bands in the PL spectrum with intensities less than 10% of the main WGMs appear probably due to the size inhomogeneities of the microspheres.

3. Effect on radiative rate

Table I gives the lifetimes and amplitudes for the CdSe coated microspheres and in colloidal solution. It can be seen that the intensity decay ($I(t)$) of colloidal QDs in toluene shows bi-exponential behaviour given by $I(t) = B_1 e^{\frac{-t}{\tau_1}} + B_2 e^{\frac{-t}{\tau_2}}$, where τ_1 and τ_2 are the decay constants and B_1 and B_2 are the corresponding amplitudes. The two lifetime components for this case are 1.01 ns and 11.32 ns, respectively. A dry thin film of QDs also gives two lifetimes as 0.60 and 3.84 ns, respectively.

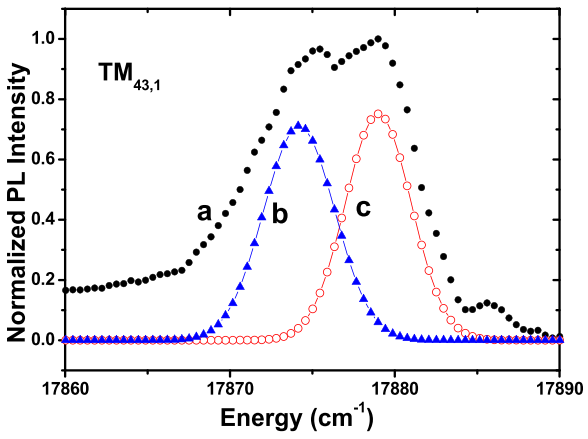

FIG. 6. Splitting observed in $TM_{43,1}$ mode (a) can be expressed with two Gaussian functions (b and c). The Q values of the two Gaussians are 3.79×10^3 (a) and 3.53×10^3 (b).

TABLE I. Lifetimes and amplitudes of CdSe QDs in solution, film, and coated on silica microcavity.

Sample	τ_1 (±0.01 ns)	τ_2 (±0.01 ns)	B_1	B_2	χ^2
QD solution	1.01	11.32	0.39	0.15	1.26
CdSe QD film	0.60	3.84	0.35	0.04	1.13
Silica microsphere (45 μm)	0.95	2.27	0.24	0.07	1.01
Silica microsphere (12 μm)	0.43				1.03

The lifetime of QDs is shorter in thin film because of inter-dot excitonic energy migration.[63] A 45 μm diameter QD coated microsphere shows faster lifetime components of 0.95 ns and 2.27 ns, respectively. Further, for a 12 μm diameter microsphere, a single exponential decay constant of 0.43 ns is obtained. It can be seen that the values of the lifetime for all the components decrease with the decrease in the microsphere size. Assuming the nonradiative rate to be constant at room temperature, we attribute this effect to the enhancement of the radiative rate in microcavities. Figure 7 gives the typical decay curves for CdSe QDs coated on single microcavity.

The Q/V_{eff} (see Eq. (4)) ratio depends nonlinearly on the microsphere size and the mode frequency.[64] The optimal radius for the maximum Q/V_{eff} can be calculated using the semi-analytical formula $r_{optimum} = 11.0 \times \lambda - 1.06$, where all units are given in μm. The maximum Q/V_{eff} occurs for a microsphere with a diameter of approximately 11 μm. In the present case, microsphere with size of 12 μm has higher Q/V_{eff} ratio compared with that of 45 μm. This is the reason for the enhancement of the radiative rate in smaller microcavities. Nevertheless, the inhibited or the bulk components may also contribute in such small particles. A trial was done to measure the decay curves at the peaks or at the valleys of the WGMs. For such measurements, the photon counting rate went down considerably when a band pass of 1 nm was chosen. The size dependence of the luminescence decay was predicted by Yokoyama-Brorson model,[42] which assumes weak coupling (Eq. (4)). Therefore, the measured decay time can be taken as the average of the modified rate for a weakly coupled system with Q-values of the order of 10^3 to 10^4. The enhancement ratio also decreases when more than one WGM mode lies within the homogenous linewidth of QDs. This also leads to the smaller rate modification in larger microspheres. Assuming the free space decay time of 11.32 ns (in solution), the enhancement factor (from Eq. (5)) for the microsphere with a diameter of 12 μm is 26.3. For these values, the approximate homogeneous line width in the PL of CdSe QDs is estimated[39] to be 7.45 cm^{-1}. This indicates that by introducing a narrow band emitter like quantum dots into a WGM resonator, it is possible to observe radiative rate modification.

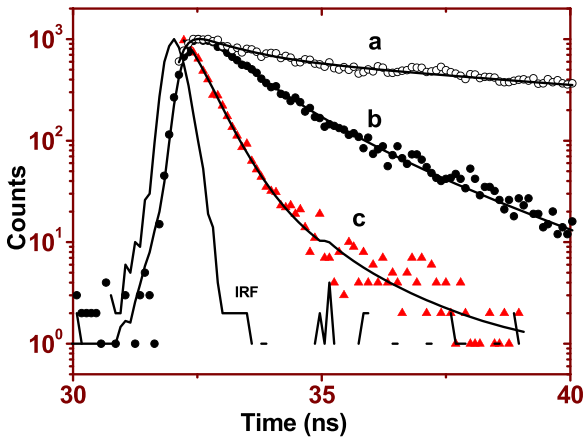

FIG. 7. Decay curves of PL of CdSe QDs in solution (a), silica microspheres with diameters of 45 μm (b) and 12 μm (c). The continuous line is the theoretical fit to the data. IRF is the instrument response function.

V. CONCLUSIONS

In conclusion, we have studied the effect of WGMs on PL of QDs coated on single silica microspheres at room temperature. The semi-classical simulations show that a nanolayer coating on a microcavity can influence the WGMs. The Q values of WGMs are enhanced on coating with a layer of high refractive index QDs. The resonance peaks shift to the lower frequency on addition of coating layer. Absorbing coatings, however, reduce the Q values of the microcavity. Experimentally observed PL spectra are modulated with the WGMs of microcavity. The positions of WGMs have been found in agreement with the simulated modes by Aden-Kerker theory. WGM splitting due to coherent coupling of the two counter propagating waves was observed in the experimental spectra. The radiative rate has been found to be enhanced in smaller WGM microcavities. The decay rates are modified due to weak coupling of the emitter and the WGMs at room temperature. This study shows that it is advantageous to use QD-coated microspheres for observing the modification of radiative rate due to photostability. Plasmonic resonances that are promising for broadband Purcell enhancement[65] also need to be mentioned here. However, their use is limited due to the intrinsic loss in the metals. On the other hand, QD embedded microcavities offer modest enhancement at sharper frequencies, which is ideal for application such as narrow linewidth microlasers.

ACKNOWLEDGMENTS

We thank Department of Science and Technology (DST), New Delhi, for financial assistance.

[1]J. Ward and O. Benson, Laser Photonics Rev. **5**(4), 553–570 (2011).
[2]M. L. Gorodetsky, A. A. Savchenkov, and V. S. Ilchenko, Opt. Lett. **21**(7), 453–455 (1996).
[3]G. S. Murugan, M. N. Zervas, Y. Panitchob, and J. S. Wilkinson, Opt. Lett. **36**(1), 73–75 (2011).
[4]J. S. Wilkinson, G. S. Murugan, D. W. Hewak, M. N. Zervas, Y. Panitchob, G. R. Elliott, P. N. Bartlett, E. J. Tull, and K. R. Ryan, in *15th European Conference on Integrated Optics (ECIO) 2010* (2010).
[5]S. Pang, R. E. Beckham, and K. E. Meissner, Appl. Phys. Lett. **92**(22), 221108 (2008).
[6]J. W. Silverstone, S. McFarlane, C. P. K. Manchee, and A. Meldrum, Opt. Express **20**(8), 8284–8295 (2012).
[7]I. Teraoka and S. Arnold, J. Opt. Soc. Am. B **23**(7), 1434–1441 (2006).
[8]J. Y. Kim, O. Voznyy, D. Zhitomirsky, and E. H. Sargent, Adv. Mater. **25**(36), 4986–5010 (2013).
[9]E. M. Purcell, H. C. Torrey, and R. V. Pound, Phys. Rev. **69**(1–2), 37–38 (1946).
[10]A. I. Ekimov, A. L. Efros, and A. A. Onushchenko, Solid State Commun. **56**(11), 921–924 (1985).

[11]L. Vorob'ev, E. Ivchenko, D. Firsov, and V. Shalygin, *Optical Properties of Nanostructures* (Nauka, Sankt-Petersburg, 2001).
[12]C. Mao, J. Qi, and A. M. Belcher, Adv. Funct. Mater. **13**(8), 648–656 (2003).
[13]J. Qi, C. Mao, J. M. White, and A. M. Belcher, Phys. Rev. B **68**(12), 125319 (2003).
[14]S. Tang, C. Mao, Y. Liu, D. Q. Kelly, and S. K. Banerjee, IEEE Trans. Electron Devices **54**(3), 433–438 (2007).
[15]A. D. Stiff, S. Krishna, P. Bhattacharya, and S. W. Kennerly, IEEE J. Quantum Electron. **37**(11), 1412–1419 (2001).
[16]P. O. Anikeeva, J. E. Halpert, M. G. Bawendi, and V. Bulović, Nano Lett. **9**(7), 2532–2536 (2009).
[17]N. N. Ledentsov, F. Hopfer, and D. Bimberg, Proc. IEEE **95**(9), 1741–1756 (2007).
[18]B. Ellis, M. A. Mayer, G. Shambat, T. Sarmiento, J. Harris, E. E. Haller, and J. Vuckovic, Nat. Photonics **5**(5), 297–300 (2011).
[19]R. E. Welser, G. G. Pethuraja, A. K. Sood, O. A. Laboutin, M. Chaplin, V. Un, W. Johnson, A. W. Sood, D. J. Poxson, J. Cho, E. F. Schubert, P. Haldar, and J. L. Harvey, "High-voltage quantum well waveguide solar cells," Proc. SPIE **8111**, 811101 (2011).
[20]P. B. Bisht, K. Fukuda, and S. Hirayama, Chem. Phys. Lett. **258**(1–2), 71–79 (1996).
[21]H. Taniguchi, S. Tanosaki, H. Yamada, T. Fujiwara, and M. Baba, J. Appl. Phys. **73**(11), 7957–7959 (1993).
[22]V. R. Dantham and P. B. Bisht, J. Opt. Soc. Am. B **26**(2), 290–300 (2009).
[23]P. Sandeep and P. B. Bisht, J. Chem. Phys. **123**(20), 204713 (2005).
[24]A. P. Alivisatos, W. Gu, and C. Larabell, Annu. Rev. Biomed. Eng. **7**(1), 55–76 (2005).
[25]N. Gaponik, Y. Rakovich, M. Gerlach, J. Donegan, D. Savateeva, and A. Rogach, Nanoscale Res. Lett. **1**(1), 68–73 (2006).
[26]Y. P. Rakovich and J. F. Donegan, Laser Photonics Rev. **4**(2), 179–191 (2010).
[27]Y. Zhi, C. P. K. Manchee, J. W. Silverstone, Z. Zhang, and A. Meldrum, Plasmonics **8**(1), 71–78 (2013).
[28]S. I. Shopova, G. Farca, A. T. Rosenberger, W. M. S. Wickramanayake, and N. A. Kotov, Appl. Phys. Lett. **85**(25), 6101–6103 (2004).
[29]J. Schäfer, J. P. Mondia, R. Sharma, Z. H. Lu, A. S. Susha, A. L. Rogach, and L. J. Wang, Nano Lett. **8**(6), 1709–1712 (2008).
[30]S. Yakunin, L. Protesescu, F. Krieg, M. I. Bodnarchuk, G. Nedelcu, M. Humer, G. De Luca, M. Fiebig, W. Heiss, and M. V. Kovalenko, Nat. Commun. **6**, 8056 (2015).
[31]P. Stehle, Phys. Rev. A **2**(1), 102–106 (1970).
[32]P. Goy, J. M. Raimond, M. Gross, and S. Haroche, Phys. Rev. Lett. **50**(24), 1903–1906 (1983).
[33]A. J. Campillo, J. D. Eversole, and H. B. Lin, Phys. Rev. Lett. **67**(4), 437–440 (1991).
[34]D. Kleppner, Phys. Rev. Lett. **47**(4), 233–236 (1981).
[35]R. G. Hulet, E. S. Hilfer, and D. Kleppner, Phys. Rev. Lett. **55**(20), 2137–2140 (1985).
[36]H. B. Lin, J. D. Eversole, C. D. Merritt, and A. J. Campillo, Phys. Rev. A **45**(9), 6756–6760 (1992).
[37]S. Ishizaka, Y. Suzuki, and N. Kitamura, Phys. Chem. Chem. Phys. **12**(33), 9852–9857 (2010).
[38]V. R. Dantham and P. B. Bisht, Eur. Phys. J.: Appl. Phys. **51**(2), 20902 (2010).
[39]P. Sandeep and P. B. Bisht, Chem. Phys. Lett. **371**(3–4), 327–332 (2003).
[40]S. Arnold, J. Chem. Phys. **106**(19), 8280–8282 (1997).
[41]H. Ikari, K. Okanishi, M. Tomita, and T. Ishidate, Opt. Mater. **30**(8), 1323–1326 (2008).
[42]H. Yokoyama and S. D. Brorson, J. Appl. Phys. **66**(10), 4801–4805 (1989).
[43]X. Fan, M. C. Lonergan, Y. Zhang, and H. Wang, Phys. Rev. B **64**(11), 115310 (2001).
[44]F. Masia, N. Accanto, W. Langbein, and P. Borri, Phys. Rev. Lett. **108**(8), 087401 (2012).
[45]N. Le Thomas, U. Woggon, O. Schöps, M. V. Artemyev, M. Kazes, and U. Banin, Nano Lett. **6**(3), 557–561 (2006).
[46]V. R. Dantham, S. Holler, C. Barbre, D. Keng, V. Kolchenko, and S. Arnold, Nano Lett. **13**(7), 3347–3351 (2013).
[47]C. E. Finlayson, P. J. A. Sazio, R. Sanchez-Martin, M. Bradley, T. A. Kelf, and J. J. Baumberg, Semicond. Sci. Technol. **21**(3), L21 (2006).
[48]M. Oxborrow, IEEE Trans. Microwave Theory Tech. **55**(6), 1209–1218 (2007).
[49]C. F. Bohren and D. R. Huffman, *Absorption and Scattering of Light by Small Particles* (John Wiley & Sons, New York, 1983).
[50]G. Mie, Ann. Phys. **330**(3), 377–445 (1908).
[51]A. L. Aden and M. Kerker, J. Appl. Phys. **22**(10), 1242–1246 (1951).
[52]R. L. Hightower and C. B. Richardson, Appl. Opt. **27**(23), 4850–4855 (1988).
[53]P. A. M. Dirac, Proc. Roy. Soc. London A **114**, 243–265 (1927).
[54]J. M. Gérard, B. Sermage, B. Gayral, B. Legrand, E. Costard, and V. Thierry-Mieg, Phys. Rev. Lett. **81**(5), 1110–1113 (1998).
[55]N. O. Anatolii, Quantum Electron. **32**(5), 377 (2002).
[56]M. Sumetsky, Y. Dulashko, and R. S. Windeler, Opt. Lett. **35**(11), 1866–1868 (2010).
[57]H. T. Beier, G. L. Coté, and K. E. Meissner, J. Opt. Soc. Am. B **27**(3), 536–543 (2010).
[58]G. C. Righini, Y. Dumeige, P. Féron, M. Ferrari, G. N. Conti, and S. S. D. Ristic, Riv. Nuovo Cimento **34**(7), 435–488 (2011).
[59]S. Chaguetmi, F. Mammeri, S. Nowak, P. Decorse, H. Lecoq, M. Gaceur, J. Ben Naceur, S. Achour, R. Chtourou, and S. Ammar, RSC Adv. **3**(8), 2572–2580 (2013).
[60]C. B. Murray, D. J. Norris, and M. G. Bawendi, J. Am. Chem. Soc. **115**(19), 8706–8715 (1993).
[61]A. L. Rogach, A. Kornowski, M. Gao, A. Eychmüller, and H. Weller, J. Phys. Chem. B **103**(16), 3065–3069 (1999).
[62]D. S. Weiss, V. Sandoghdar, J. Hare, V. Lefèvre-Seguin, J. M. Raimond, and S. Haroche, Opt. Lett. **20**(18), 1835–1837 (1995).
[63]C. R. Kagan, C. B. Murray, and M. G. Bawendi, Phys. Rev. B **54**(12), 8633–8643 (1996).
[64]I. H. Agha, J. E. Sharping, M. A. Foster, and A. L. Gaeta, Appl. Phys. B **83**(2), 303–309 (2006).
[65]G. M. Akselrod, C. Argyropoulos, T. B. Hoang, C. Ciracì, C. Fang, J. Huang, D. R. Smith, and M. H. Mikkelsen, Nat. Photonics **8**(11), 835–840 (2014).